Received: 19 December 2018 | Revised: 27 September 2019 | Accepted: 3 October 2019

DOI: 10.1002/asl.940

RESEARCH ARTICLE

Atmospheric Science Letters RMetS

Time series analysis of normal mode energetics for Rossby wave breaking and saturation using a simple barotropic model

Takumi Matsunobu[1] | **Hiroshi L. Tanaka**[2]

[1]Graduate School of Life and Environmental Sciences, University of Tsukuba, Tsukuba, Ibaraki, Japan

[2]Center for Computational Sciences, University of Tsukuba, Tsukuba, Ibaraki, Japan

Correspondence
Hiroshi L. Tanaka, Center for Computational Sciences, University of Tsukuba, Tsukuba, Ibaraki 305-8577, Japan.
Email: tanaka@ccs.tsukuba.ac.jp

Funding information
Japan Society for the Promotion of Science, Grant/Award Number: KAKENHI JP17K05651

Abstract

In this study, Rossby wave breaking and saturation are examined for an idealized situation using a simple barotropic spectral model. In the model, a Rossby wave is amplified by parameterized baroclinic instability. The increase of the wave energy stops at the level where the high and low potential vorticities (PVs) indicate overturning, which is equivalent to the fact that the meridional PV gradient becomes negative somewhere in the domain. In this study, it is shown theoretically that the criterion may be represented by the point when the wave energy exceeds a quarter of the originally proposed saturation level specified by $E = (p_s/g)c^2$ in the spectral domain, by assuming a sinusoidal curve for the wave. Rossby wave saturation under the new definition proposed in this study could be followed by wave breaking, which occurs when the energy level of the background noise becomes comparable to that of harmonic waves of the amplified unstable wave. It is found that the criterion of PV overturning is equivalent to the energy level of wave saturation, and wave breaking is a distinct phenomenon from wave saturation.

KEYWORDS

barotropic model, dynamic/processes, normal mode energetics, Rossby wave, wave breaking, wave saturation

1 | INTRODUCTION

Rossby wave breaking has long been studied as a trigger of many characteristic phenomena, such as stratospheric sudden warming (Matsuno, 1971), a formation and maintenance of blocking (Shutts, 1983), or a formation of cut-off low associated with extreme precipitation (Enomoto *et al.*, 2003). For example, a dipole blocking in a westerly flow may be understood as a persistent meridional overturning of high and low potential vorticity (PV) as discussed by Tanaka (1998).

In Garcia (1991), the criterion was expressed by the following equation using PV q as:

$$\frac{\partial q}{\partial y} < 0, \tag{1}$$

namely, meridional gradient of PV becomes negative somewhere in the domain due to overturning of q. This criterion is physically reasonable in reference to the necessary condition for barotropic or baroclinic instability (Charney and Stern, 1962).

The Garcia's criterion was examined by Tanaka and Watarai (1999), using a simple barotropic spectral model. According to their result, amplified Rossby wave reached to the saturation point, where the wave energy will be dissipated at a rate just to prevent further energy growth. Yet, the subsequent wave breaking did not occur for the entire period

of the experiment (200 days) despite the appearance of negative PV gradients. They suggested that the wave saturation and wave breaking are distinctly different phenomena. They proposed not only the negative PV gradient but also the increase of eddy energies of all individual wavenumbers are the necessary condition for a wave breaking.

The Garcia (1991)'s criterion is transformed to a new criterion for the upper bound of an energy level in a phase speed c-domain, where the horizontal wave scale is represented by the Rossby wave phase speed c (Tanaka *et al.*, 2004). In their study, the criterion was expressed as

$$E < \frac{p_s}{g} c^2, \tag{2}$$

where E is total energy of a normal mode, p_s is mean surface pressure, g is acceleration of gravity, and c is a phase speed of a Rossby wave appearing in Hough functions of a normal mode energetics. A phase speed c of a Rossby wave is represented by σ/n: the eigenfrequency of the Laplace's tidal equation σ divided by the zonal wavenumber n in shallow water system on a sphere. Since the eigenfrequencies σ are different depending on horizontal wavenumber n and meridional modes l, $c = \sigma/n$ are varying with different couple of n and l. Tanaka *et al.* (2004) also showed the energy spectrum in the c-domain obeys the c^2 spectral slope, and they defined this criterion as the Rossby wave saturation point. Although the time mean energy spectrum in the phase speed c-domain was clearly elucidated by this Rossby wave breaking criterion, the time evolution of the energy spectrum and the formation of the energy saturation spectrum in the c-domain was not examined by previous studies.

In this study, the criteria for Rossby wave breaking and saturation are examined using a simple barotropic spectral model used by Tanaka and Watarai (1999). We investigate a sequence of the Rossby wave amplification by the baroclinic instability, Rossby wave saturation, and Rossby wave breaking to form the energy spectrum in the c-domain. The formation of the energy spectrum obeying the c^2 power law as geostrophic turbulence is examined in reference to the Rossby wave saturarion and breaking criterion.

2 | EXPERIMENTAL METHODS

2.1 | Governing equations

The governing equations and model descriptions in this study are presented in detail by Tanaka and Watarai (1999). A brief description of the model is presented here. The governing equations used in this study are the primitive equations in spherical coordinates. The primitive equations may be reduced to a vector equation, written as

$$M\frac{\partial U}{\partial t} + \mathrm{LU} = N + F, \tag{3}$$

where state variables are

$$U = (u, v, \phi)^T. \tag{4}$$

The symbols u, v, *and* ϕ are zonal and meridional components of wind velocity and a departure of the geopotential from the global mean, respectively, and the superscript T represents a transpose, and t represents time. Matrices M and L are vertical and horizontal differential operators, N and F are nonlinear term vector and forcing term vector, respectively.

Assuming a resting basic state for (3), we can obtain three-dimensional (3D) normal mode functions Π_{nlm} (λ, θ, p), defined as a tensor product of vertical normal modes and horizontal normal modes of Hough harmonics. By expanding U and F in the orthonormal basis of the 3D normal mode functions, we can obtain a system of 3D spectral primitive equations in terms of the spectral expansion coefficients w_i of the state variables:

$$\frac{dw_i}{d\tau} + i\sigma_i w_i = -i\sum_{j=1}^{K}\sum_{k=1}^{K} r_{ijk}\, w_j\, w_k + f_i, i = 1, 2, \cdots, K, \tag{5}$$

$f_i = (\mathrm{DF})_i + (\mathrm{BC})_i + (\mathrm{SF})_i$, where τ is a dimensionless time, σ_i is an eigenfrequency of the Laplace's tidal equation, r_{ijk} is an interaction coefficient for nonlinear wave–wave interactions, K is a number of terms in the series expansion, and f_i is an external forcing. The symbol i in the equation is the imaginary unit, and the subscripts i, j, and k represent 3D wavenumber that combines a set of zonal wavenumber n, meridional mode number l, vertical mode number m into one symbol. The 3D spectral model of (5) is then truncated by rhomboidal 20 for n and l using only symmetric Rossby modes about the equator (about 1,000 × 1,000 km grid). We use only the component of $m = 0$ to construct a barotropic model similar to a shallow water equation on a sphere. We consider a diffusion, baroclinic instability *BC*, and surface friction *SF* for the external forcing. Refer to Tanaka and Watarai (1999) for the details of *DF* and *SF*. The parameterization of *BC* is described in the next section.

2.2 | Parameterization of baroclinic instability

In order to parameterize the process of baroclinic instability, we linearize the 3D baroclinic spectral model using a zonal basic state, and solve the eigenvalue problem to obtain the most unstable mode of the baroclinic instability. The equation for the first order term of an inviscid and adiabatic perturbation becomes

$$\frac{dw_i'}{d\tau} + i\sigma_i w_i' = -i\sum_{j=1}^{K}\left(\sum_{k=1}^{K}(r_{ijk}+r_{ikj})\overline{w_k}\right)w_j', i = 1,2,\cdots,K, \tag{6}$$

where $\overline{w_k}$ is a time-independent zonal basic state, and w_j' is a perturbation from the basic state. We use the winds and geopotential height of the January climate state for 50 years mean by NCEP/NCAR reanalysis data (Kalnay *et al*., 1996) as the zonal basic state. Then we can solve the eigenvalue problem for each zonal wavenumber n to get the solutions below:

$$w_i'(\tau) = \zeta_i \exp(-i\nu\tau) \tag{7}$$

where an eigenvalue ν and an eigenvector ξ_i are complex numbers. The eigenvector ξ_i represents the structure of baroclinic instability, and the real and imaginary parts of ν represent the frequency and growth rate of baroclinically unstable modes. We can define the following parameterization for the baroclinic instability:

$$(\mathrm{BC})_i = \begin{cases} -i(\nu_R + i\alpha\nu_I)a(\tau)\xi_i \ (n = n_s), \\ 0 \ (n \neq n_s), \end{cases} \tag{8}$$

where $\nu = \nu_\mathrm{R} + \nu_\mathrm{I}$, and $a(\tau)$ is an amplitude of the unstable mode, and n_s is a specific zonal wavenumber amplified as a wavemaker in each experiment. In this model, the state variable of w_i is projected on to the most unstablemode ξ_i to get the amplitude $a(\tau)$ in the barotropic component of the atmosphere. Since $a(\tau)$ is a time-dependent function of $w_i(\tau)$, $(\mathrm{BC})_i$ is also a time-dependent function (see Tanaka and Watarai (1999)).

We used α as a scaling factor to control the growth rate for different experiments as in Tanaka and Watarai (1999). By this scheme, the state variable is amplified toward the direction of the unstable mode ξ_i by the amount of the total growth rate $\alpha\nu_I$ at every timestep. We used the same governing equations and a parameterization scheme as in Tanaka and Watarai (1999) where the basic state of a specific winter of the First Global Atmospheric Research Program Global Experiment data were used.

2.3 | Defining the Rossby wave saturation theory

In Tanaka *et al*. (2004), the saturated energy spectrum E in the phase speed c domain is found to obey the slope of c^2 with a multiple constant of p_s/g. Since the energy spectrum was explained by the Rossby wave saturation with the energy source of baroclinic instability, the theory was referred to as Rossby wave saturation theory (Terasaki and Tanaka, 2007). This theory is quite different from the traditional inertial subrange theory for turbulence where no energy source is assumed in the inertial subrange.

In the Rossby wave saturation theory, the exponential growth of eddy wind speed u is bounded by c, as derived by the condition $\frac{\partial q}{\partial y} < 0$. Therefore, the total energy E which is sum of potential energy and vertical mean kinetic energy $\frac{u^2+v^2}{2}$ of growing eddy is bounded by $E < \frac{p_s}{g}c^2$ in the shallow water system. In the shallow water system, PV is derived as below:

$$q = \frac{\zeta + f}{h_0 + z}, \tag{9}$$

where ζ is relative vorticity, f is planetary vorticity, h_0 is the equivalent height and $z = \phi/g$ is geopotential height deviation from the mean.

In the original theory by Tanaka *et al*. (2004), they assumed that both u and v are bounded by c to derive the above equation of saturation criterion. It may be shown, however, that the criterion should be multiplied by 1/4 when a sinusoidal wave is assumed for u and v in the calculation of mean energy. Therefore, the saturation condition should be redefined as below:

$$E < \frac{p_s}{4g}c^2. \tag{10}$$

3 | RESULTS OF THE EXPERIMENTS

The model Equation (5) is integrated from an initial value of a white noise spectrum as shown in Figure 4a superimposed on a zonal wind of January climate. The energy level of the initial white noise is about 1 Jm^{-2} for each eddy. The initial zonal wind is the barotropic component of the basic state used in Section 2.2. The baroclinic instability is imposed only at the zonal wavenumber $n_s = 6$.

First, we set the scaling factor α as 1.3 to amplify the wavenumber 6 and run the model for 1,000 days. We call this experiment as Exp. 1. Figure 1 illustrates the distribution of shallow water PV (contour) and negative gradient of shallow water PV (shaded) in the Northern Hemisphere over 20°N for days 0, 16, 35, and 1,000. The structure of wavenumber 6 is strongly amplified, and negative PV gradient appears by day 16 around 40°N (Figure 1b), but the structure is maintained even for 1,000 days (Figure 1d). This result agrees with the weakly nonlinear equilibrium demonstrated by Tanaka and Watarai (1999) where the energy supply by the baroclinic instability at $n_s = 6$ has balanced with the frictional dissipation by the wavemaker $n = 6$ and its

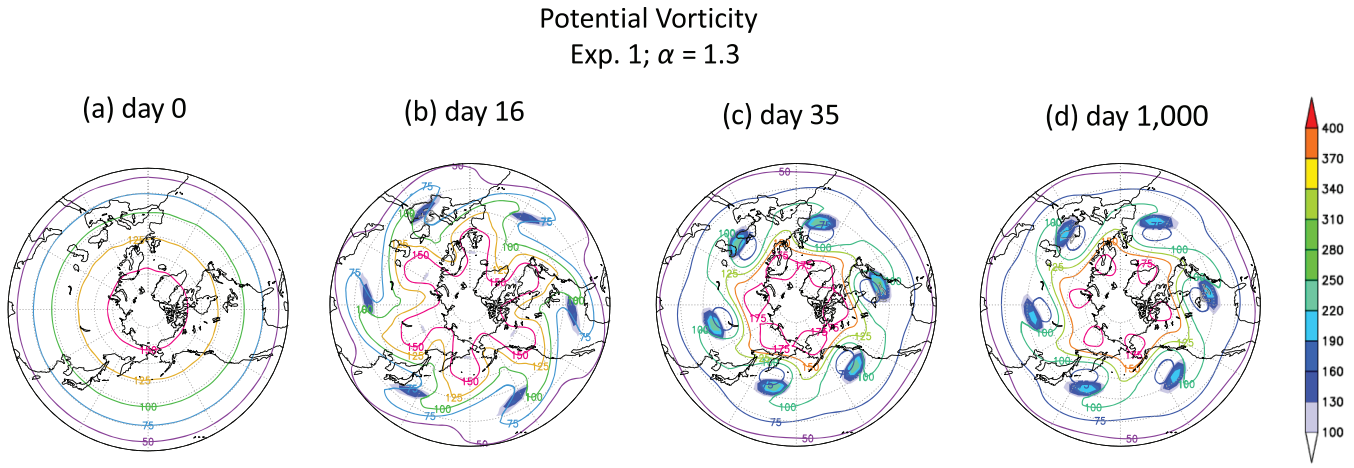

FIGURE 1 Distribution of shallow water potential vorticity (10^{-10} m^{-1} s^{-1}) (contour) and negative shallow water PV gradient (10^{-10} m^{-2} s^{-1} degree^{-1}) (shaded) in the northern hemisphere for days 0, 16, 35, and 1,000 for Exp. 1. Contours are drawn at every 25×10^{-10} m^{-1} s^{-1}. The structure of wave 6 is maintained until 1,000 days

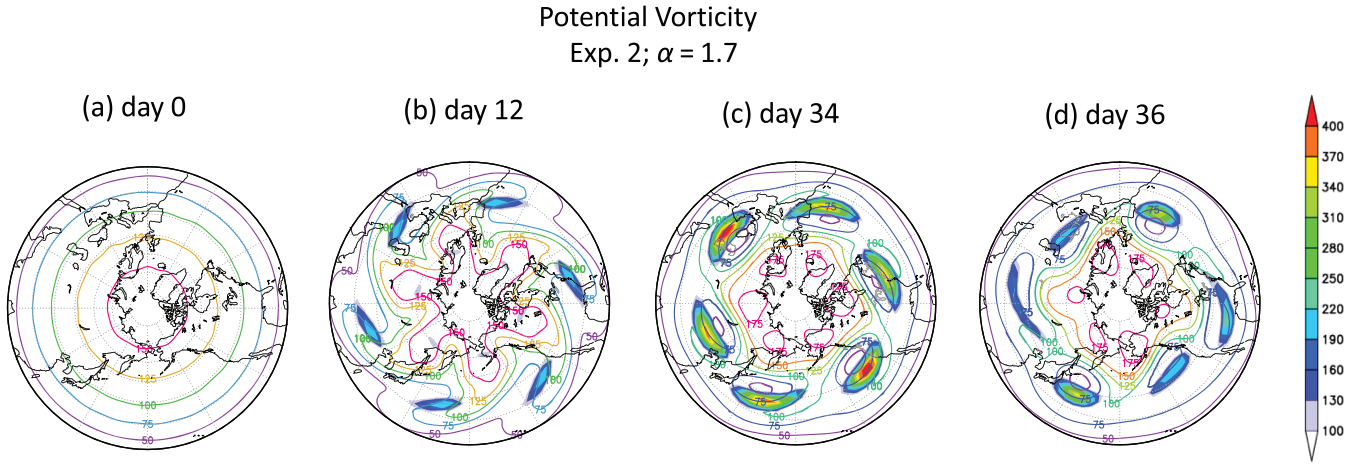

FIGURE 2 As in Figure 1, but for days 0, 12, 34 and 36 for Exp.2. The waves had broken down between days 34 and 36

harmonic waves of $n = 12$, and 18. The noise energy for wavenumbers other than 6, 12, and 18 are not amplified until the end of the simulation period.

Next, we conducted a similar experiment Exp. 2 with the scaling factor $\alpha = 1.7$, keeping other parameters same as Exp. 1. Figure 2 shows the PV distributions for days 0, 12, 34, 36. Owing to the larger αv_I, the wavenumber 6 is amplified faster than Exp. 1, and negative PV gradient appears by day 12 (Figure 2b). The wavenumber 6 structure is maintained during day 12 to day 34. The structure had been broken by day 36 (Figure 2d). In Exp.1 the exponential growth terminates when the meridional overturning of PV occurred. In this study, we define the appearance of negative PV gradient as wave saturation and consider it not as the wave breaking, although the wave breaking has been defined for the overturning of PV in the previous literature.

In Figure 3, energy of the amplified wave grows exponentially at the first stage with a simultaneous growth of wavemaker and its harmonic waves. In the following, energy of the amplified wave implies the sum of the wavemaker (n_s= 6) and its harmonics (n_s = 12 and 18). For both Exps, negative PV gradient appears for the first time when the energy of the amplified wave exceeds the $E = \frac{p_s}{4g} c^2$ line, and the exponential growth stopped at the day 19 and day 14 for Exp. 1 and 2, respectively, when the energy levels have reached the $E = \frac{p_s}{g} c^2$ line. In Exp.2, the energy slightly overshoots the $E = \frac{p_s}{g} c^2$ line, then dropped to a lower level. The energy supply by the baroclinic instability stops when the meridional overturning of PV occurs, so the energy can exceed the theoretical upper limit for a snapshot. The energies of amplified wave hover around the modified energy level of the saturation, $E = \frac{p_s}{4g} c^2$, after the energy peaks. This

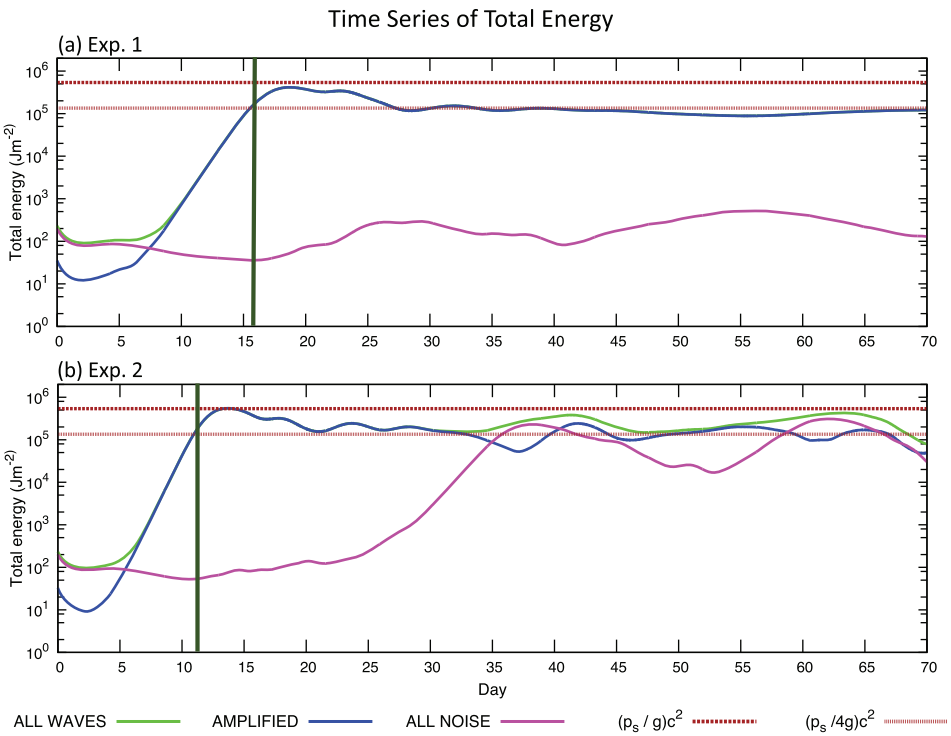

FIGURE 3 The time series of a total energy of all wave (green), the amplified waves (blue), and other noise waves (pink) for Exp.1 (upper) and Exp.2 (lower). The horizontal dashed (upper) and dotted (lower) lines show the $E = (p_s/ g)\, c^2$ and the $E = (p_s/4\ g)\, c^2$ level of all the $n = 6$ modes, respectively. The vertical line (dark) shows the day when the negative PV gradient appears for the first time around 40° N in the PV map for each experiment

saturation level seems to relate to the appearance of the negative PV gradient, and the originally proposed saturation level $E = \frac{p_s}{g} c^2$ seems to relate to the energy peaks. This result is consistent with the theoretical derivation of $E = \frac{p_s}{g} c^2$ that shows $E = \frac{p_s}{g} c^2$ is equivalent to upper bound of wind speed and kinetic energy. Hence, we can confirm that the negative PV gradient could work as the criterion of Rossby wave saturation.

In Exp. 2, the noise energy exceeds the amplified wave energy around the day 35, crossing the two lines in time series (Figure 3b). This crossing does not occur in Exp. 1. In this special case, the amplified Rossby wave has been saturated, but has not been broken, maintaining the predominant zonal wavenumber 6. It is inferred that the crossing of amplified wave energy and noise energy is suitable for a definition of wave breaking in this study. The results agree with the criterion discussed in Tanaka and Watarai (1999). The energy transfer from the wavemaker to noise energy by the strong nonlinear interactions plays a key role for the criterion of the wave breaking. We repeated the same numerical experiments 20 times using slightly different initial conditions, and found the conclusion is robust for all experiments (not shown).

Figure 4 shows a time sequence of the energy spectrum in the phase speed c-domain for Exp. 2 at days 0, 10, 12, and 36. On day 0, all the modes have energy around 1 Jm^{-2} indicating a white noise spectrum (Figure 4a). Then energy is injected by the forcing of baroclinic instability and redistributed to other waves by wave–wave interactions, while it is dissipated by diffusion at short waves (Figure 4b). On day 12, the energy levels for some large scale meridional modes of $n = 6$ have reached and exceeded the saturation line in the c-domain. Since the wave $n = 6$ is continuously amplified by the baroclinic instability, the energy spectrum for $n = 6$ overshoots the saturation line indicating the spectrum of baroclinic instability rather than a turbulence spectrum. The energy levels for noise are smaller than the $E = \frac{p_s}{4g} c^2$ line (Figure 4c), showing that only wavenumber 6 has developed. It is shown by the numerical experiment that the theoretical saturation line agrees quantitatively well with the saturation spectrum for the amplified waves. On day 36, just after the wave breaking in the PV maps, noise energy has increased and finally reached the saturation line (Figure 4d).

In this experiment with the wavemaker only at $n_s = 6$, synoptic-scale waves obey the saturation energy spectrum, but the energy levels for short waves are much smaller than the saturation level. Since the accumulated energy cascades up to the Rhines scale for two-dimensional (2D) turbulence (Tanaka *et al.*, 2004), we need to consider sufficient energy source at short waves to meet with the saturation line for all the spectral range. It should be noted that the saturation energy spectrum for short waves would obey the theoretical line when a sufficient energy supply is considered for this range. According to the normal mode energetics with a very high horizontal resolution of Japan Meteorological Agency global analysis, the saturation energy spectrum is shown to obey the theoretical saturation line up to the wavenumber 250 (Terasaki *et al.*, 2011).

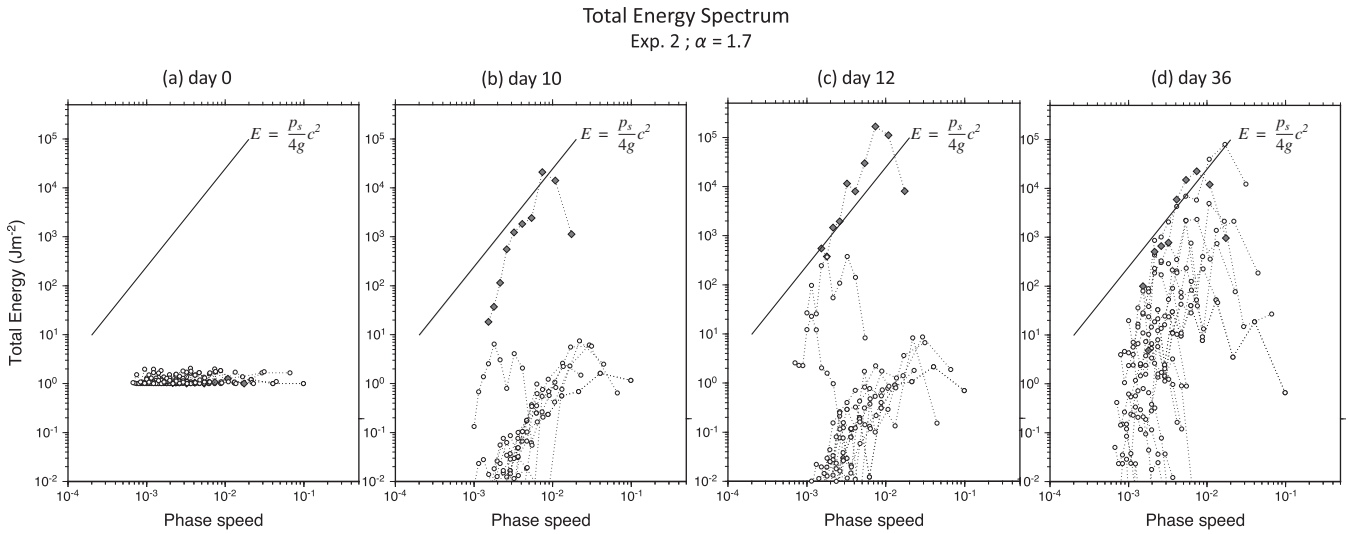

FIGURE 4 The normal mode energy spectra in the dimensionless phase-speed c-domain for days 0, 10, 12, and 36 for Exp. 2. Different meridional modes l with the same n are connected by dotted lines, and the points for wave 6 are filled with black. The straight line shows the modified energy saturation level of $E = (p_s/4\ g)\ c^2$ derived in this study

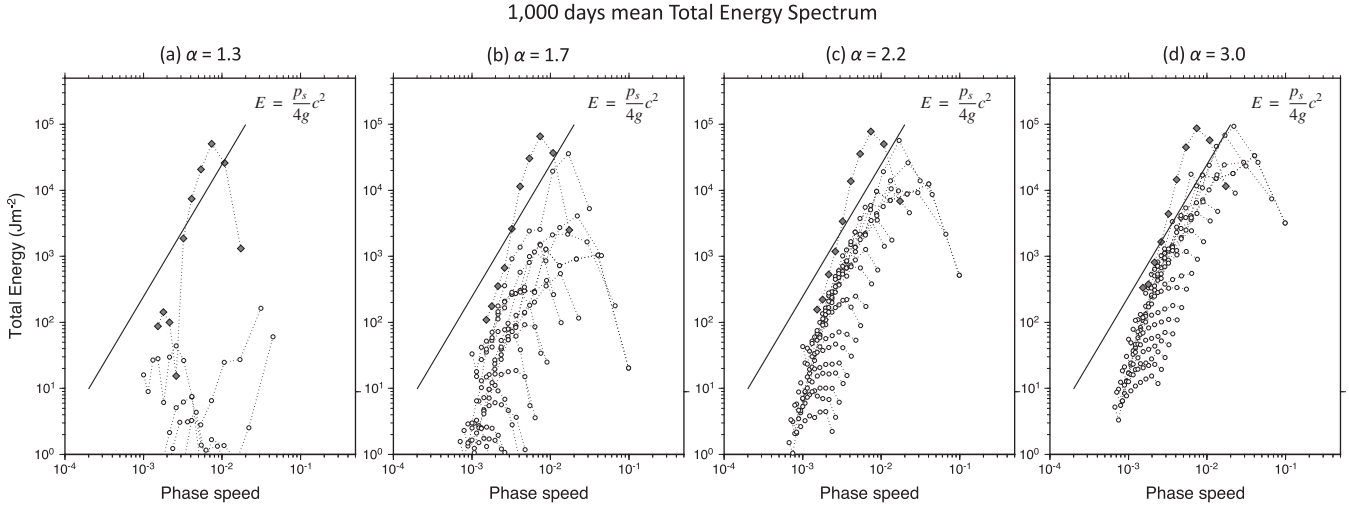

FIGURE 5 As in Figure 4, but for the 1,000 days mean energy levels for experiments with α = 1.3, 1.7, 2.2, and 3.0

Figure 5 shows same energy spectrum but for 1,000 days means for the experiments with scaling factors $\alpha = 1.3$, 1.7, 2.2, and 3.0, respectively. In this figure, the energy levels for $n = 6$ (black dots) are located along the theoretical saturation line although they are overshot slightly. Noise energy of other waves are obviously supplied by the amplified wave of $n = 6$. The energy levels for short waves are low because there is no energy source in this range as mentioned in the previous paragraph. According to the Rossby wave saturation theory, the increased energy level by baroclinic instability is saturated at the theoretical saturation level of $E = \frac{p_s}{4g} c^2$, which is equivalent to the appearance of the meridional overturning of PV in the PV map. If there is an energy source at short waves, we can expect the same saturation theory to hold for short wave.

The energy levels of the amplified waves and noise increase with increasing α in average, and they gradually approach the saturation line. However, they have not exceeded the saturation line even for a very large scaling factor $\alpha = 3.0$. This shows that the saturation level is not determined by the scaling factor of baroclinic instability, but by the appearance of the meridional overturning of PV. It seems reasonable to suggest that the theoretical saturation line is a function only of the phase speed of Rossby wave as denoted by $E = \frac{p_s}{4g} c^2$.

We also conducted similar experiments with the wavemaker at different zonal wavenumbers of $n_s = 3$, 4, 8, 10, 12 (not shown). In these experiments, we set various scaling factors for each wavemaker. It is found that the same results of energy slope, wave saturation and wave breaking

are obtained for $n_s = 3$, 4 and 8. Yet, the results for $n_s = 10$ and 12 show less up-scale energy cascade to planetary waves due to the insufficient model resolution. Energy spectrum appears to be less steeper than that of the saturation line. Despite the difference in the slope of energy spectra, the PV gradient becomes negative when the energy reaches $E = \frac{p_s}{4g} c^2$, and the wave breaking occurs when noise energy exceeds that of the amplified waves as demonstrated by other experiments.

4 | CONCLUDING SUMMARY

In this study, the criteria for Rossby wave breaking and saturation are examined in the view of the time evolution for an idealized numerical experiments using a simple barotropic general circulation model. In the model, a Rossby wave is amplified by parameterized baroclinic instability. In this study, numerical experiments are conducted for various parameter settings of wavemaker at the zonal wavenumber 6 to analyze the time evolution of unstable waves to form the saturation energy spectrum.

As a result, it is found that Garcia's criterion for wave breaking $\frac{\partial q}{\partial y} < 0$ is in fact a criterion for wave saturation in the aspect of time series. The exponential growth of eddy energy must terminate at the saturation level of $E = \frac{p_s}{g} c^2$, which is equivalent to the Garcia's criterion in the c-domain, where c is the normal mode phase speed of Rossby wave. In this study, the theoretical saturation level is modified as $E = \frac{p_s}{4g} c^2$, assuming a sinusoidal wave for eddies. We found that negative PV gradient appears when the eddy energy overshoots the modified saturation level, and then the energy hovers around this level, and the excess energy is transferred to back ground noise energy by the nonlinear wave–wave interactions.

It is found that a Rossby wave breaking occurs when the energy of noise exceeds that of the amplified waves. In the PV map, the amplified Rossby wave breaks down, showing a turbulence-like mixing of PV. We find in their time series that the Rossby wave saturation is followed by the Rossby wave breaking, and these two are distinctly different processes.

By present study we find that the turbulence energy spectrum in the c-domain can be explained by the Rossby wave saturation theory. This theory is different from the traditional theory of the inertial subrange in that the energy source exists everywhere in the domain, mostly by the baroclinic instability. In order for the saturation energy spectrum to follow the theoretical saturation line in the c-domain, it is also found that certain energy source is required at the short waves because energy mostly cascades up to large scale in the 2D turbulence. We also conducted the similar experiments with other wavemakers. This theory is reinforced by the results with large-scale wavemakers $n_s = 3$, 4 and 8. Such a source of energy in short waves is an important research subject in the future.

The sequence of the normal mode energetics for breaking Rossby waves in the c-domain may be summarized as follows: First, the synoptic waves are amplified exponentially by baroclinic instability. The harmonic waves are immediately amplified by weakly nonlinear interactions. When the amplified wave has reached at the theoretical saturation line, it transfers the excessive energy to the back ground noise by the strong nonlinear interactions. An overturning of PV occurs in the PV map and the exponential growth by the linear instability terminates. Then, the noise energy increases rapidly, and it soon becomes comparable to the energy level of the amplified wave. Finally, the amplified Rossby wave breaks down, showing a turbulence-like mixing of PV. Eventually, the up-scale energy cascade for 2D turbulence transfers the excessive energy to the Rhines scale obeying the energy saturation line in the c-domain as shown by Tanaka *et al.* (2004).

This process is governed by the nonlinear wave–wave interactions of eddies, which is explained by the Rossby wave saturation theory. Therefore, the traditional theory of inertial subrange for geostrophic turbulence must be updated by this alternative theory.

ACKNOWLEDGEMENTS

This work was supported by Japan Society for the Promotion of Science KAKENHI Grant Number JP17K05651. The authers are thankful to the two anonymous reviewers whose comments helped improve the quality of this paper.

ORCID

Takumi Matsunobu https://orcid.org/0000-0001-5178-2098
Hiroshi L. Tanaka https://orcid.org/0000-0002-2769-3631

REFERENCES

Charney, J.G. and Stern, M.E. (1962) On the stability of internal baroclinic jets in a rotating atmosphere. *Journal of the Atmospheric Sciences*, *19*, 159–172.

Enomoto, T., Hoskins, B.J. and Matsuda, Y. (2003) The formation mechanism of the bonin high in august. *Quarterly Journal of the Royal Meteorological Society*, *129*, 157–178.

Garcia, R.R. (1991) Parameterization of planetary wave breaking in the middle atmosphere. *Journal of the Atmospheric Sciences*, *48*, 1405–1419.

Kalnay, E., Kanamitsu, M., Kistler, R., Collins, W., Deaven, D., Gandin, L., Iredell, M., Saha, S., White, G., Woollen, J., Zhu, Y., Chelliah, M., Ebisuzaki, W., Higgins, W., Janowiak, J., Mo, K.C., Ropelewski, C., Wang, J., Leetmaa, A., Reynolds, R., Jenne, R.

and Joseph, D. (1996) The NCEP/NCAR 40-year reanalysis project. *Bulletin of the American Meteorological Society*, *77*, 437–472.

Matsuno, T. (1971) A dynamical model of the stratospheric sudden warming. *Journal of the Atmospheric Sciences*, *28*, 1479–1494.

Shutts, G.J. (1983) The propagation of eddies in diffluent jetstreams: Eddy vorticity forcing of "blocking" flow fields. *Quarterly Journal of the Royal Meteorological Society*, *109*, 737–761.

Tanaka, H.L. (1998) Numerical simulation of a life-cycle of atmospheric blocking and the analysis of potential vorticity using a simple barotropic model. *Journal of the Meteorological Society of Japan*, *76*, 983–1008.

Tanaka, H.L. and Watarai, Y. (1999) Breaking Rossby waves in the barotropic atmosphere with parameterized baroclinic instability. *Tellus A*, *51*, 552–573.

Tanaka, H.L., Watarai, Y. and Kanda, T. (2004) Energy spectrum proportional to the squared phase speed of Rossby modes in the general circulation of the atmosphere. *Geophysical Research Letters*, *31*, L13109.

Terasaki, K. and Tanaka, H.L. (2007) Barotropic energy spectrum by the Rossby wave saturation in the zonal wavenumber domain. *SOLA*, *3*, 25–28.

Terasaki, K., Tanaka, H.L. and Žagar, N. (2011) Energy spectra of Rossby and gravity waves. *SOLA*, *7*, 45–48.

How to cite this article: Matsunobu T, Tanaka HL. Time series analysis of normal mode energetics for Rossby wave breaking and saturation using a simple barotropic model. *Atmos Sci Lett*. 2019;20:e940. https://doi.org/10.1002/asl.940